LIMP-2 expression is critical for β-glucocerebrosidase activity and α-synuclein clearance

Michelle Rothaug[a,1], Friederike Zunke[a,1], Joseph R. Mazzulli[b], Michaela Schweizer[c], Hermann Altmeppen[d], Renate Lüllmann-Rauch[e], Wouter W. Kallemeijn[f], Paulo Gaspar[g], Johannes M. Aerts[f], Markus Glatzel[d], Paul Saftig[a], Dimitri Krainc[b], Michael Schwake[a,h], and Judith Blanz[a,2]

[a]Institute of Biochemistry and [e]Anatomical Institute, Christian Albrechts University of Kiel, 24098 Kiel, Germany; [b]Department of Neurology, Northwestern University Feinberg School of Medicine, Chicago, IL 60611; [c]Department of Electron Microscopy, Centre for Molecular Neurobiology, and [d]Institute of Neuropathology, University Medical Centre Hamburg-Eppendorf, 20246 Hamburg, Germany; [f]Department of Medical Biochemistry, Academic Medical Centre, University of Amsterdam, 1105 AZ Amsterdam, The Netherlands; [g]Unidade de Biologia do Lisossoma e do Peroxissoma, Instituto de Biologia Molecular e Celular, 4150-180 Porto, Portugal; and [h]Faculty of Chemistry/Biochemistry III, University of Bielefeld, 33615 Bielefeld, Germany

Edited by Thomas C. Südhof, Stanford University School of Medicine, Stanford, CA, and approved September 15, 2014 (received for review April 4, 2014)

Mutations within the lysosomal enzyme β-glucocerebrosidase (GC) result in Gaucher disease and represent a major risk factor for developing Parkinson disease (PD). Loss of GC activity leads to accumulation of its substrate glucosylceramide and α-synuclein. Since lysosomal activity of GC is tightly linked to expression of its trafficking receptor, the lysosomal integral membrane protein type-2 (LIMP-2), we studied α-synuclein metabolism in LIMP-2–deficient mice. These mice showed an α-synuclein dosage-dependent phenotype, including severe neurological impairments and premature death. In LIMP-2–deficient brains a significant reduction in GC activity led to lipid storage, disturbed autophagic/lysosomal function, and α-synuclein accumulation mediating neurotoxicity of dopaminergic (DA) neurons, apoptotic cell death, and inflammation. Heterologous expression of LIMP-2 accelerated clearance of overexpressed α-synuclein, possibly through increasing lysosomal GC activity. In surviving DA neurons of human PD midbrain, LIMP-2 levels were increased, probably to compensate for lysosomal GC deficiency. Therefore, we suggest that manipulating LIMP-2 expression to increase lysosomal GC activity is a promising strategy for the treatment of synucleinopathies.

SCARB2 | AMRF | PME | GD | C57/BL6-J

The lysosomal integral membrane protein type-2 (LIMP-2) is the receptor for lysosomal transport of the acid hydrolase β-glucocerebrosidase (GC) (1) catalyzing the intralysosomal degradation of the sphingolipid glucosylceramide (GluCer). Mutations within the gene encoding LIMP-2 (SCARB2, scavenger receptor B2) cause action myoclonus renal failure syndrome (AMRF) (2, 3), a progressive myoclonic epilepsy (PME) associated with renal failure, ataxia, the presence of undefined storage material in the brain, and premature death. LIMP-2–deficient (LIMP-$2^{-/-}$) mice (4) are a valid disease model for AMRF. To date, several SCARB2 mutations have been identified in AMRF, as well as in some PME cases (5, 6). AMRF/PME mutants mislocalize to the endoplasmic reticulum (ER) and fail to transport GC to lysosomes (7, 8). The crystal structure of the ectodomain of LIMP-2 highlights a helical bundle in LIMP-2 as the GC binding site (9).

Mutations in GBA1, the gene encoding GC, lead to Gaucher disease (GD), a lysosomal storage disorder that has been linked to Parkinson disease (PD) (10). LIMP-2 has been identified as a modifier for the neurological presentation of GD (11). The neuropathological hallmark of PD and other synucleinopathies is Lewy bodies (LBs) that contain aggregated α-synuclein (α-syn). LBs can also be found in brains of patients with GD (12), who have about a 20-fold increased risk of developing PD. In transgenic and pharmacological [conduritol β-epoxide (CBE)] induced GD mice, a reduction in GC activity leads to accumulation of different soluble and insoluble α-syn species (13–15), whereas adenoviral overexpressed GC lowered α-syn levels in transgenic mouse models of GD and PD (16). Moreover, recent data suggest that accumulated α-syn disrupts ER/Golgi trafficking of GC, resulting in a positive feedback loop that amplifies the pathological effects of α-syn (14). Because trafficking of GC requires LIMP-2 (1) and genetic variations within the LIMP-2 locus have been linked to PD and dementia with LBs (17–19), we were prompted to examine the role of LIMP-2 in α-syn aggregation.

Results

α-Syn Accumulates in the Brainstem of LIMP-$2^{-/-}$ Mice. Previously, the presence of undefined storage material in the brain, ataxia, slight hyperactivity, and a normal life span have been reported for LIMP-$2^{-/-}$ mice (3). However, these mice were maintained in a mixed genetic background (SVJ129-C57/BL6-J), including the 6J strain from Harlan Laboratories, which is deficient for α-syn (20), suggesting that the observed pathology (summarized in Fig. S1*A*) was not related to α-syn. Immunoblots of brain material (Fig. 1*A*) showed reduced or complete absence of α-syn in mice of the mixed background (SVJ129-C57/BL6-J) compared with C57/BL6-N mice. This result is in agreement with quantitative RT-PCR analysis, which showed reduced amounts of α-syn mRNA in SVJ129-C57/BL6-J animals (Fig. 1*B*), whereas LIMP-2

Significance

Our report highlights, for the first time to our knowledge, a distinct relationship between lysosomal integral membrane protein type-2 (LIMP-2) expression, β-glucocerebrosidase (GC) activity, and clearance of α-synuclein. In LIMP-2–deficient mice, increased levels of endogenous α-synuclein led to severe neurological deficits and premature death. We found that loss of LIMP-2 reduced lysosomal GC activity, resulting in lipid storage, disturbed autophagic/lysosomal function, and α-synuclein accumulation leading to neurotoxicity of dopaminergic neurons as well as apoptotic cell death and inflammation. Furthermore, heterologous overexpression of functional LIMP-2 enhanced α-synuclein clearance and improved lysosomal activity of GC. Our results suggest that lysosomal GC activity can be influenced via its interaction with LIMP-2, which could be a promising strategy for the treatment of synucleinopathies.

Author contributions: M.R., F.Z., J.R.M., P.S., D.K., M. Schwake, and J.B. designed research; M.R., F.Z., J.R.M., M. Schweizer, H.A., R.L.-R., W.W.K., P.G., M. Schwake, and J.B. performed research; J.M.A., M.G., P.S., and D.K. contributed new reagents/analytic tools; M.R., F.Z., J.R.M., M. Schweizer, H.A., P.S., D.K., M. Schwake, and J.B. analyzed data; and M.R., F.Z., D.K., M. Schwake, and J.B. wrote the paper.

The authors declare no conflict of interest.

This article is a PNAS Direct Submission.

[1]M.R. and F.Z. contributed equally to this work.

[2]To whom correspondence should be addressed. Email: jblanz@biochem.uni-kiel.de.

This article contains supporting information online at www.pnas.org/lookup/suppl/doi:10.1073/pnas.1405700111/-/DCSupplemental.

NEUROSCIENCE

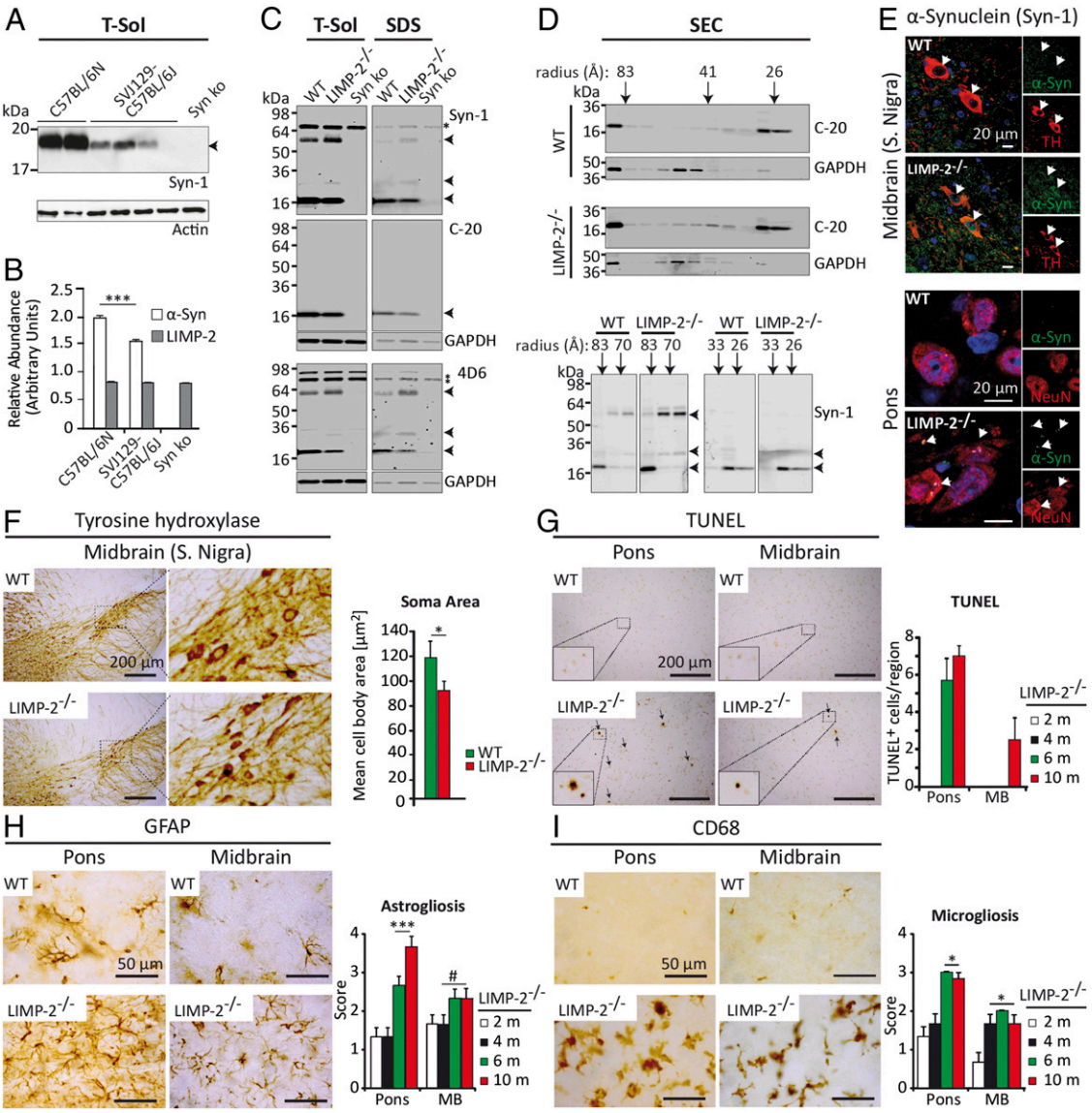

Fig. 1. Accumulation of α-syn, apoptosis, and gliosis in LIMP-2$^{-/-}$ brain. Immunoblot of α-syn (*A*) and quantitative RT-PCR of α-syn and LIMP-2 (*B*) from brain samples of mice with different genetic backgrounds. (*C*) Immunoblots of α-syn in wild-type (WT) and LIMP-2$^{-/-}$ soluble (T-Sol) and insoluble (SDS) fractions of midbrain (arrowheads indicate α-syn species, and the asterisk indicates a nonspecific band; GAPDH was used to control loading). (*D*) Native SEC/immunoblot analysis of T-Sol lysates (radius in angstroms). GAPDH was used as a loading control. (*E*) Immunofluorescent staining of α-syn (green) colabeled with NeuN (red) and TH (red) in the pons and midbrain of 10-month-old littermates (arrowheads highlight accumulated α-syn). S. Nigra, substantia nigra. (*F*) Quantification of the soma area of DAB-stained TH-positive neurons within the S. Nigra (WT, $n = 3$; LIMP-2$^{-/-}$, $n = 4$). Quantification and representative DAB staining from 10-month-old mice show TUNEL-positive apoptotic cells (*G*; arrows), astrogliosis (*H*; GFAP), and microgliosis (*I*; CD68) in LIMP-2$^{-/-}$ mice but not in WT mice (also Fig. S1). m, months of age. $^{\#}P > 0.05$; $^{*}P < 0.05$; $^{***}P < 0.001$.

mRNA levels remained unchanged. α-Syn was not detectable in BL6-J [α-syn-deficient (Syn ko)] mice, confirming the specificity of the applied probes. After LIMP-2$^{-/-}$ animals were backcrossed into C57/BL6-N mice that express normal levels of α-syn, they showed reduced weight when compared to wild type (WT) (WT: 34.2 ± 5.4 g, LIMP-2$^{-/-}$: 22.2 ± 2.8 g; $P < 0.001$ at 10 months) and did not survive beyond 10 months. From 4 months of age, backcrossed LIMP-2$^{-/-}$ mice presented with severe neurological impairments, such as tremor and hind-limb clasping, which progressed to partial paralysis (Fig. S1*B*).

In immunoblots of Triton-soluble (T-Sol) and insoluble (SDS) fractions prepared from WT and LIMP-2$^{-/-}$ midbrain, we identified different α-syn species using three different antibodies [Syn-1 (BD Biosciences), 4D6 (Abcam), and C-20 (Santa Cruz Biotechnology)] migrating at around 17, 23, and 58 kDa that were not present in Syn ko mice (Fig. 1*C*). Although levels of monomeric α-syn were unchanged in T-Sol fractions of LIMP-2$^{-/-}$ tissue and slightly decreased in SDS fractions of LIMP-2 tissue (Fig. 1*C* and Fig. S1 *C* and *D*), the 23-kDa and 58-kDa forms of α-syn were elevated in both fractions (Syn-1, 4D6). We next used native size exclusion chromatography (SEC), followed by SDS-PAGE/immunoblotting of the collected fractions, to assess the presence of T-Sol oligomeric α-syn species. A higher proportion of α-syn within high-molecular mass fractions was evident after detection with two separate antibodies (Syn-1 and C-20) in LIMP-2$^{-/-}$ samples (Fig. 1*D*). Accumulation of α-syn in the pons and midbrain, including the substantia nigra, was confirmed by immunofluorescence (Fig. 1*E* and Fig. S1 *H* and *I*) and DAB (3,3′ diaminobenzidine) immunohistochemistry (Fig. S1 *G–I*) using the Syn-1, 4D6, and C20 antibodies. Double

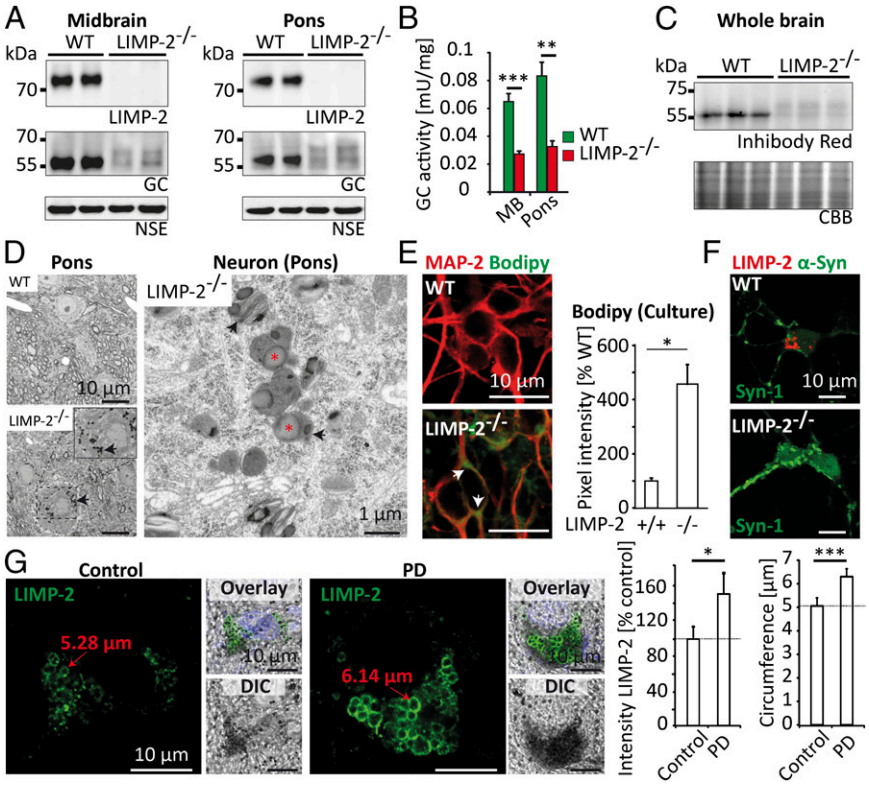

Fig. 2. Reduced GC activity accompanied by lipid accumulation and lysosomal dysfunction. Reduced GC protein levels and enzyme activity in LIMP-2$^{-/-}$ midbrain, pons, and whole-brain lysates assessed by immunoblot analysis (*A*), activity assay (*B*), and Inhibody Red staining (*C*) [neuron-specific enolase (NSE) or Coomassie Brilliant Blue (CBB) was used to control loading]. (*D*) Ultrastructural analysis of the pons. Toluidine blue-stained sections of neurons (arrows highlight storage material) are shown. Electron micrographs show electron-dense rich deposits (arrows) and lipid droplets (red asterisks) within the soma of a LIMP-2$^{-/-}$ neuron. Accumulation of Bodipy 493/503-stained lipid droplets (green, arrows) within the soma of MAP-2–labeled neurons (red) (*E*) that show increased levels of α-syn (green) in the absence of LIMP-2 (red) (*F*) is illustrated. (*G*) Immunological staining of LIMP-2 (green) and respective densitometric analysis in PD and control midbrain sections identified via their high neuromelanin content [black structures in differential interference contrast (DIC) image]. The circumference of a randomly chosen lysosome is highlighted in each sample, and the total intensity of the LIMP-2 signal per cell was quantified and divided by the area of the cell to compensate for variation in cell size (also Fig. S2). $*P < 0.05$; $**P < 0.01$; $***P < 0.001$.

immunofluorescence of α-syn with the neuronal marker NeuN in the pons (Fig. 1*E* and Fig. S1 *H* and *I*) and the dopaminergic (DA) marker tyrosine-hydroxylase (TH) within the substantia nigra (Fig. 1*E*) showed accumulation of α-syn in the soma of these neurons. The specificity of the applied α-syn antibodies was validated in WT and Syn ko sections (Fig. S1 *E* and *F*). These results suggest that neuronal accumulation of α-syn contributed to the pathological phenotype observed in LIMP-2$^{-/-}$ mice.

α-Syn–Mediated Neurotoxicity in LIMP-2$^{-/-}$ Brains. Accumulation of α-syn mediates neurotoxicity in cell and animal models, especially within DA neurons that undergo neurodegeneration in PD (14, 21). Compared with WT, TH-labeled neurons within the substantia nigra of LIMP-2$^{-/-}$ brains were significantly shrunken in size, suggestive of degeneration (Fig. 1*F*). TUNEL staining of brain sections from mice at different ages revealed progressive apoptotic cell death in the pons and midbrain of LIMP-2$^{-/-}$ animals (Fig. 1*G*). Astrogliosis and microgliosis are commonly observed in PD mouse models and in patients with PD. Therefore, we used DAB immunohistochemistry on brain sections with astrocyte (GFAP) (Fig. 1*H*) and microglia (macrosialin/CD68) (Fig. 1*I*) markers. The pons and midbrain of 2-, 4-, 6-, and 10-month-old LIMP-2$^{-/-}$ mice displayed a progressively increasing number of GFAP- and CD68-positive cells. In addition, numerous CD68-positive microglial cells exhibited a plump and amoeboid shape, indicating activation. In summary, we conclude that increased expression of α-syn in combination with LIMP-2 deficiency within the C57/BL6-N genetic background led to significant α-syn–dependent neurodegeneration of DA neurons, apoptotic cell death, gliosis, and CNS impairments.

Reduced GC Activity in LIMP-2$^{-/-}$ Brains Accompanied by Lipid Accumulation and Lysosomal/Autophagic Dysfunction. Since expression of LIMP-2 and GC is tightly linked (1, 7), we hypothesized that a reduction in GC could contribute to the observed α-syn pathology in LIMP-2$^{-/-}$ brains. Immunoblot analysis of LIMP-2$^{-/-}$ pons and midbrain lysates (Fig. 2*A*) showed strong reduction in GC protein levels accompanied by a significant decline in GC activity (Fig. 2*B*), whereas mRNA levels were unchanged (Fig. S2*A*). Using a recently described Inhibody probe that specifically labels active GC (22), a significant reduction of active enzyme was confirmed in LIMP-2–deficient brains (Fig. 2*C*).

Our findings of reduced GC activity in LIMP-2$^{-/-}$ brain prompted us to assess the potential accumulation of its substrate, GluCer, in LIMP-2$^{-/-}$ neurons. Toluidine blue-stained sections revealed accumulation of storage material within LIMP-2$^{-/-}$ neurons of the pons but not in WT cells (Fig. 2*D*). Ultrastructural analysis revealed the presence of electron-dense material, lipid droplets, and lamellated bodies (Fig. 2*D*, *Right*). To identify the accumulated substrate, periodic acid–Schiff stain (PAS) was applied to brain sections. PAS labels tissue carbohydrates and has been used to identify Gaucher cells, which accumulate high amounts of GluCer (23). PAS staining displayed progressive storage of carbohydrate conjugates, particularly in the pons of LIMP-2$^{-/-}$ mice (Fig. S2*B*). Staining of primary cultured neurons with the fluorophore Bodipy 493/503 (Invitrogen), which was previously used to assess GluCer storage (14), showed accumulation of Bodipy-positive droplets in the soma and neurites of LIMP-2$^{-/-}$, but not in WT neurons (Fig. 2*E*), suggesting intracellular accumulation of GluCer. We also found significant accumulation of vesicular α-syn in the soma and proximal neurites of LIMP-2$^{-/-}$ neurons (Fig. 2*F*), indicating an association between these two pathological events.

Because LIMP-2 and GC are functionally linked, and loss of GC activity leads to lysosomal dysfunction, we postulated that LIMP-2$^{-/-}$ mice will exhibit changes in lysosomal activity. Therefore, we tested expression and/or activity of three different lysosomal hydrolases. Immunoblot analysis of LIMP-2$^{-/-}$ brain lysates revealed increased levels and impaired maturation of cathepsin D in the midbrain and pons (Fig. S2*D*). The activities of β-hexosaminidase and α-mannosidase were also increased

(Fig. S2*C*). Furthermore, we examined expression of p62, an adaptor protein that targets cellular cargo to autophagosomes for lysosomal degradation. Morphologically, we observed comparable accumulation of p62 in LIMP-2$^{-/-}$ midbrain and pons in 2-, 4-, and 10-month-old mice (Fig. S2*E*). A marked increase in insoluble p62 was observed in immunoblots from LIMP-2$^{-/-}$ brains (Fig. S2*F*). We therefore suggest that loss of LIMP-2 expression leads to alterations in the autophagy/lysosome system that could possibly lead to accumulation of α-syn.

Thus, we analyzed potential alterations of LIMP-2 levels in midbrain neurons of patients with PD. In order to accurately quantify LIMP-2 levels in DA neurons of synucleinopathy cases ($n = 5$) and appropriate controls ($n = 7$), we have used LIMP-2 immunofluorescence and confocal laser scanning microscopy of postmortem midbrain samples. A similar approach has been used by other groups investigating expression of the lysosomal protein Park9/ATP13A2 in human synucleinopathies (24–26). Nonspecific binding of the LIMP-2 antibody in DA neurons was controlled using another rabbit-IgG antibody (Fig. S2*G*). Furthermore, specificity of the LIMP-2 antibody is demonstrated by the absence of signal in fibroblasts from patients with AMRF (Fig. S2*I*), which do not show detectable LIMP-2 in immunoblot analysis (Fig. S2*J*) due to the absence of the epitope recognized by our antibody (Fig. S2*H*). In alkaline phosphatase red-stained sections, LIMP-2 expression was evident in DA neurons within human midbrain from controls and patients with PD (Fig. S2*K*). In the brain of patients with PD, substantial loss of DA neurons, as reported by others (27), was apparent. Using immunofluorescence, we observed increased expression of LIMP-2 in the soma of surviving DA neurons in PD brains, as well as an enlargement of LIMP-2–positive vesicles compared with controls (Fig. 2*G*). In the brain of patients with PD, LIMP-2 levels were still increased when measuring LIMP-2–specific fluorescence within the lysosomal membrane of individual lysosomes, which was normalized to vesicle size (Fig. S2*L*), further suggesting that LIMP-2 plays a role in regulating lysosomal function in PD.

LIMP-2 Overexpression Increases Clearance of α-Syn and Lysosomal GC Activity. Our data point to an important role for LIMP-2 in regulating α-syn levels. To elucidate if an increase in LIMP-2 expression is beneficial for α-syn homeostasis, both proteins were coexpressed in different cellular systems, including neuronal cell lines. Heterologous expression of WT LIMP-2 but not ER-retained LIMP-2 (LIMP-2 ERret), which prevents lysosomal localization of LIMP-2 (1), led to a significant reduction in α-syn protein but not mRNA levels (Fig. 3*A* and Fig. S3*A*) in the murine neuroblastoma cell line N2a. Endoglycosidase H (EndoH) digestion of N2a lysates, used to distinguish between ER (EndoH-sensitive) and post-ER (EndoH-insensitive) forms of GC, showed a significant increase in the post-ER/ER GC ratio upon overexpression of WT but not LIMP-2 ERret (Fig. S3*B*), which was accompanied by augmented GC activity (Fig. 3*B*). Analysis of single clones from murine fibroblasts stably expressing LIMP-2 and α-syn revealed a dose-dependent effect of LIMP-2 expression on trafficking of GC to post-ER compartments and on α-syn steady-state levels (Fig. S3*D*). To address the turnover rate of α-syn, depending on expression of LIMP-2, we used human neuroglioma H4 cells, expressing α-syn under the control of a tetracycline-inducible promoter (14). Overexpression of LIMP-2 significantly decreased α-syn levels and increased trafficking of GC to post-ER compartments (Fig. 3*C*). The same effect was observed in HeLa cells (Fig. S3*C*). To study α-syn clearance in the presence of LIMP-2, H4 cells were transfected with either an empty vector (mock) or human LIMP-2 cDNA and simultaneously treated with doxycycline to suppress α-syn transcription. The expression of LIMP-2 after 24 h accelerated clearance of α-syn from this point (Fig. 3*D* and Fig. S3*E*). In a comparable setup, a significant difference in clearance of α-syn after 72 h of doxycycline treatment and LIMP-2 expression was observed (Fig. S3 *F* and *G*). Our data suggest that overexpression of LIMP-2 accelerates the intralysosomal degradation of α-syn by increasing lysosomal activity of GC.

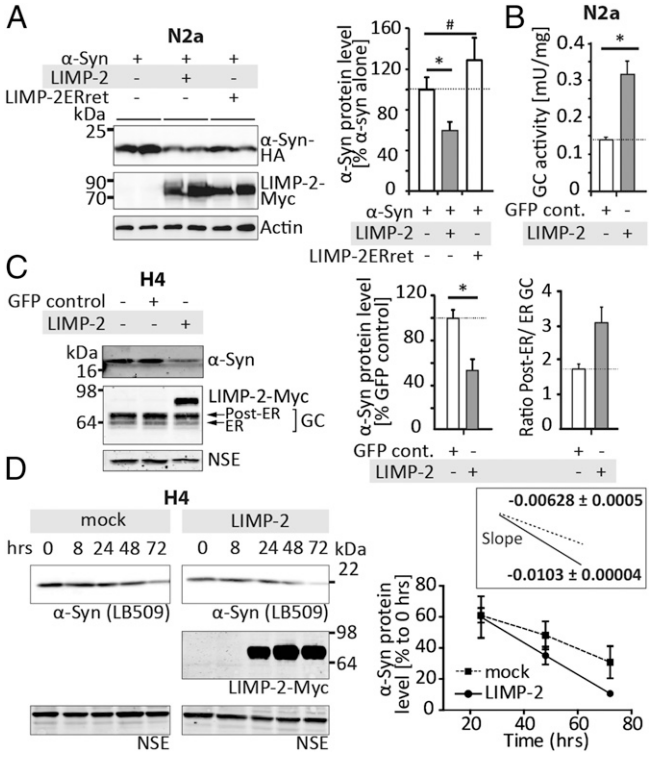

Fig. 3. Heterologous overexpression of LIMP-2 is beneficial for α-syn clearance. (*A*) Immunoblotting and densitometry of HA-tagged α-syn (α-syn-HA) in N2a cells after overexpression of LIMP-2 or LIMP-2 ERret. (*B*) GC activity assay of N2a cells with GFP control (GFP cont.) or overexpressed LIMP-2. (*C*) Immunoblot and densitometry of α-syn and post-ER/ER GC levels in H4 cells after 48 h of LIMP-2 overexpression. (*D*) Immunoblot and densitometry of α-syn turnover in H4 cells after treatment with doxycycline to suppress further α-syn transcription. Enhanced clearance of α-syn is highlighted with the larger absolute value of the slope compared with a mock-transfected control (also Fig. S3). $^{\#}P > 0.05$; $^{*}P < 0.05$.

Discussion

The current report highlights a distinct relationship between LIMP-2 expression and α-syn accumulation. The presence of increased levels of endogenous α-syn mRNA and protein levels in LIMP-2$^{-/-}$ mice backcrossed into C57/BL6-N mice led to severe neurological deficits and premature death in contrast to LIMP-2–deficient mice bred in the α-syn–deficient background, clearly suggesting a link between disease severity and α-syn dosage. A dosage relationship between α-syn and disease progression is consistent with recent reports showing that transgenic overexpression of murine WT α-syn exacerbates the neurological phenotype (28, 29). These reports are also in agreement with some cases of familial PD, where duplications or triplications of the SNCA gene lead to Lewy pathology and disease onset that correlates with α-syn expression (30). Conversely, reduction of endogenous α-syn in neurotoxin-based PD mouse models dramatically reduces behavioral phenotypes, protein accumulation, and neuronal death (31, 32). The phenotype of LIMP-2$^{-/-}$ C57/BL6-N mice, including motor deficits, hind-limb paralysis, weight loss, and premature death, resembles transgenic PD mouse models expressing mutant A53T α-syn (33, 34), further suggesting that the observed neuropathology is related to α-syn accumulation. In addition to α-syn, we cannot rule out other

genetic differences between the two substrains that might have an impact on the severity of the disease observed in our mouse model after backcrossing. To elucidate whether loss of LIMP-2 in humans leads to comparable accumulation of α-syn, analysis of postmortem AMRF brains for α-syn pathology will be of interest. AMRF patient fibroblasts expressing dysfunctional LIMP-2 show loss of lysosomal GC and reduced enzyme activity (2) (Fig. S2*J*). Therefore, it is likely that a significant reduction in lysosomal GC activity contributes to the neuropathology in AMRF brains, including α-syn accumulation.

Our biochemical data suggest that LIMP-2 depletion resulted in accumulation of soluble and insoluble oligomeric α-syn species in LIMP-2$^{-/-}$ brain. This increase in α-syn was likely due to lysosomal deficiency of GC and subsequent accumulation of its lipid substrates (14). Loss-of-function GBA1 mutations have been associated with a higher risk of developing PD (10), and recent research of autopsy cases of patients with sporadic PD showed reduced GC activity in brain regions with increased α-syn levels (35, 36). These findings are consistent with previous data in cell and mouse models demonstrating that GC loss of function induced α-syn accumulation in vitro and in vivo (13–15, 37, 38). However, at this stage, we cannot rule out any direct effect of LIMP-2 on α-syn metabolism independent of its function as a GC transporter. Further studies on transgenic mice expressing a LIMP-2 mutant incapable of binding GC but still trafficked correctly to the lysosome would help to elucidate the specific role of LIMP-2 in α-syn metabolism.

Several other hypotheses suggest a link between GC mutations and α-syn accumulation (10). For example, mutant GC localizes to LBs (39) and has been shown to interact directly with α-syn (40). Another group identified impaired ER-associated degradation (ERAD) by the mutated enzyme (41). However, such hypotheses cannot explain the occurrence of PD in patients with GD with null mutations (42) or the in vivo accumulation of α-syn after CBE injection (13, 15) and in LIMP-2$^{-/-}$ mice. Our data suggest that loss of GC function, not through GBA1 mutations but through trafficking deficits of WT GC, resulted in α-syn accumulation and neurotoxicity. In contrast to GD mouse models, LIMP-2$^{-/-}$ mice provide a unique tool to assess what influence a significant reduction of lysosomal GC activity has on the accumulation of α-syn without affecting ERAD through the expression of toxic GC mutants or reducing the activity of several other hydrolases through hypomorphic expression of prosaposin (15, 43).

The autophagy/lysosomal pathway is implicated in clearance of aggregated proteins in neurodegenerative diseases, such as PD (44). The importance of the lysosomal pathway in PD is highlighted by the fact that mutations in the lysosomal protein ATP13A2/PARK9 lead to early-onset parkinsonism, pyramidal degeneration, and dementia (Kufor–Rakeb syndrome) (45, 46). Depletion of ATP13A2 in neurons and in mutant human fibroblasts affects lysosomal function, including impaired maturation of cathepsin D, resulting in neuronal accumulation of endogenous α-syn (25, 47). Cathepsin D is important for α-syn degradation (48), and increased protein levels were found in brains of patients with sporadic PD (36). In the present study, we also report elevated cathepsin D levels in LIMP-2$^{-/-}$ pons and midbrain, which have not been observed in the α-syn–deficient background (1), supporting the suggested function of this protease for α-syn clearance. Increased lysosomal enzyme activity, as well as impaired maturation of cathepsin D and accumulation of p62, signifies a relationship between perturbed autophagic/lysosomal function and α-syn clearance in LIMP-2$^{-/-}$ mice, as suggested for mouse models of neuronopathic GD (49) and PD (25, 47).

In support of this hypothesis, we found increased levels of LIMP-2 in enlarged lysosomes of surviving DA neurons within the midbrain of patients with PD. This increase could be a compensatory measure to overcome impaired targeting of GC to the lysosome due to accumulated α-syn, and could therefore protect neurons from α-syn toxicity. A similar up-regulation as a protective mechanism is also discussed for other PD-linked lysosomal proteins, such as ATP13A2/Park9 in neurons that are exposed to pathologically accumulated α-syn (26). Our data are in conflict with the data of Gegg et al. (35), who did not report changes in immunoblot levels of LIMP-2 in PD midbrain lysates. This discrepancy may be due to either the use of different brain material or the method applied, because we have analyzed individual neurons of PD midbrain and not the entire cellular content. Clearly, further studies in PD brains will be required to address this question.

Genetic variations (SNPs) of LIMP-2 have been linked to PD (17, 18); however, this finding is somewhat controversial (50). Therefore, further validation of LIMP-2 mutations on a larger cohort of patients with PD will be required. A recent report describing a significant association of the SCARB2 locus with dementia with LBs supports our findings of synucleinopathy in murine brain lacking LIMP-2 (19).

Our data suggest that LIMP-2 expression can modify α-syn pathogenesis and point out the significance of functional LIMP-2 for the outcome of therapeutic strategies that target GC. Indeed, introduction of WT GC into GD and PD mouse models (16) ameliorated α-syn–mediated CNS impairments, highlighting the importance of GC function for PD progression. This hypothesis is supported by our in vitro studies, which demonstrate a beneficial effect of overexpressed LIMP-2 on lysosomal transport of GC and α-syn clearance potentially by reducing lysosomal GluCer levels, and thus abolishing its effect on α-syn and lysosomal function. The possibility to reduce α-syn in such a manner has potential therapeutic value, especially for studies that focus on improved translocation of GC to lysosomes, because LIMP-2 may be limiting in this process.

Experimental Procedures

Experimental Animals and Primary Cultures. LIMP-2$^{-/-}$ mice have been previously described (4) and were backcrossed three to seven times into C57BL/6-N mice (Charles River Laboratories). C57BL/6-J mice (Harlan Laboratories; Syn ko), were used to control α-syn antibody and quantitative RT-PCR probe specificity. All experiments were carried out under guidelines set by the National Animal Care Committee (Ministry of Energy, Agriculture, the Environment and Rural Areas, Schleswig-Holstein). Siblings from either sex were used for analysis, and each experiment was performed with a minimum of three animals per genotype. Due to increased mortality from 10 months onward, mice were prepared at or before this age. A detailed description of primary cultures can be found in *SI Experimental Procedures*.

Histology, EM, Immunoblotting, Indirect Immunofluorescence, Bodipy 493/503 Staining, and Heterologous Expression. A detailed outline of the antibodies used and a description of mouse tissue preparation for histological and ultrastructural analysis, as well as immunoblotting, indirect immunofluorescence, and heterologous expression, can be found in *SI Experimental Procedures*. Paraffin sections were prepared from postmortem midbrain of patients with PD and controls (patients with PD: $n = 5$, aged 61–88 y; controls: $n = 7$, aged 61–87 y). A detailed description of morphometric analyses can be found in *SI Experimental Procedures*.

Sequential Detergent Fractionation of Mouse Brain, Enzyme Activity Assays, SEC, Inhibody Gels, and Western Blotting. Sequential extraction of soluble and insoluble proteins, as well as SEC, was carried out as described by Mazzulli et al. (14). Lysosomal enzyme activity was determined according to the method of Blanz et al. (51). GC activity was measured as described by Reczek et al. (1) and activity inhibited by CBE was assigned as specific for GC. Inhibody labeling was carried out according to Witte et al. (22). Samples were normalized to the respective loading controls [actin, neuron-specific enolase (NSE), GAPDH, or tubulin] and presented as protein levels relative to WT.

Plasmids and Cell Lines. cDNA for α-syn (Thermo Scientific) was cloned into the pcDNA3.1 Hygro^{+} vector (Invitrogen). Expression plasmids of LIMP-2 and the ER retention mutant (LIMP-2 ERret) were generated previously (1).

Statistical Analyses. All values are expressed as the mean ± SEM and are analyzed via a two-tailed, unpaired Student *t* test with Microsoft Excel software or one-way ANOVA, followed by a Tukey–Kramer or Bonferroni multiple comparison test using GraphPad Instat 3 software where applicable.

In all analyses, the null hypothesis was rejected at $P < 0.05$ ($^{\#}P > 0.05$; $^{*}P < 0.05$; $^{**}P < 0.01$; $^{***}P < 0.001$).

ACKNOWLEDGMENTS. We thank M. Senkara, L. Andresen, M. Langer, and S. Jeon for excellent technical assistance and S. Berkovic (University of Melbourne, Australia) for the AMRF fibroblasts. This work was supported by Research Training Group Grant GRK1459 of the Deutsche Forschungsgemeinschaft (DFG) (to J.B., M.G., and M. Schwake), DFG Grant Schw 866/4-1 (to M. Schwake), European Union Grant EU/ALPHA-MAN 261331 (to P.S. and J.B.), a Boehringer Ingelheim Fonds grant (to F.Z.), National Institutes of Health Grant R01NS076054 (to D.K.), and Fundação para a Ciência e Tecnologia Grant SFRH/BD/72862/2010 (to P.G.).

1. Reczek D, et al. (2007) LIMP-2 is a receptor for lysosomal mannose-6-phosphate-independent targeting of beta-glucocerebrosidase. *Cell* 131(4):770–783.
2. Balreira A, et al. (2008) A nonsense mutation in the LIMP-2 gene associated with progressive myoclonic epilepsy and nephrotic syndrome. *Hum Mol Genet* 17(14): 2238–2243.
3. Berkovic SF, et al. (2008) Array-based gene discovery with three unrelated subjects shows SCARB2/LIMP-2 deficiency causes myoclonus epilepsy and glomerulosclerosis. *Am J Hum Genet* 82(3):673–684.
4. Gamp AC, et al. (2003) LIMP-2/LGP85 deficiency causes ureteric pelvic junction obstruction, deafness and peripheral neuropathy in mice. *Hum Mol Genet* 12(6): 631–646.
5. Dibbens LM, et al. (2009) SCARB2 mutations in progressive myoclonus epilepsy (PME) without renal failure. *Ann Neurol* 66(4):532–536.
6. Fu YJ, et al. (2014) Progressive myoclonus epilepsy: Extraneuronal brown pigment deposition and system neurodegeneration in the brains of Japanese patients with novel SCARB2 mutations. *Neuropathol Appl Neurobiol* 40(5):551–563.
7. Blanz J, et al. (2010) Disease-causing mutations within the lysosomal integral membrane protein type 2 (LIMP-2) reveal the nature of binding to its ligand beta-glucocerebrosidase. *Hum Mol Genet* 19(4):563–572.
8. Zachos C, Blanz J, Saftig P, Schwake M (2012) A critical histidine residue within LIMP-2 mediates pH sensitive binding to its ligand β-glucocerebrosidase. *Traffic* 13(8): 1113–1123.
9. Neculai D, et al. (2013) Structure of LIMP-2 provides functional insights with implications for SR-BI and CD36. *Nature* 504(7478):172–176.
10. Westbroek W, Gustafson AM, Sidransky E (2011) Exploring the link between glucocerebrosidase mutations and parkinsonism. *Trends Mol Med* 17(9):485–493.
11. Velayati A, et al. (2011) A mutation in SCARB2 is a modifier in Gaucher disease. *Hum Mutat* 32(11):1232–1238.
12. Wong K, et al. (2004) Neuropathology provides clues to the pathophysiology of Gaucher disease. *Mol Genet Metab* 82(3):192–207.
13. Manning-Boğ AB, Schüle B, Langston JW (2009) Alpha-synuclein-glucocerebrosidase interactions in pharmacological Gaucher models: A biological link between Gaucher disease and parkinsonism. *Neurotoxicology* 30(6):1127–1132.
14. Mazzulli JR, et al. (2011) Gaucher disease glucocerebrosidase and α-synuclein form a bidirectional pathogenic loop in synucleinopathies. *Cell* 146(1):37–52.
15. Xu YH, et al. (2011) Accumulation and distribution of α-synuclein and ubiquitin in the CNS of Gaucher disease mouse models. *Mol Genet Metab* 102(4):436–447.
16. Sardi SP, et al. (2013) Augmenting CNS glucocerebrosidase activity as a therapeutic strategy for parkinsonism and other Gaucher-related synucleinopathies. *Proc Natl Acad Sci USA* 110(9):3537–3542.
17. Do CB, et al. (2011) Web-based genome-wide association study identifies two novel loci and a substantial genetic component for Parkinson's disease. *PLoS Genet* 7(6): e1002141.
18. Hopfner F, et al. (2013) The role of SCARB2 as susceptibility factor in Parkinson's disease. *Mov Disord* 28(4):538–540.
19. Bras J, et al. (2014) Genetic analysis implicates APOE, SNCA and suggests lysosomal dysfunction in the etiology of dementia with Lewy bodies. *Hum Mol Genet*, 10.1093/hmg/ddu334.
20. Specht CG, Schoepfer R (2001) Deletion of the alpha-synuclein locus in a subpopulation of C57BL/6J inbred mice. *BMC Neurosci* 2:11.
21. Periquet M, Fulga T, Myllykangas L, Schlossmacher MG, Feany MB (2007) Aggregated alpha-synuclein mediates dopaminergic neurotoxicity in vivo. *J Neurosci* 27(12): 3338–3346.
22. Witte MD, et al. (2010) Ultrasensitive in situ visualization of active glucocerebrosidase molecules. *Nat Chem Biol* 6(12):907–913.
23. Adachi Y, et al. (1998) An autopsy case of fetal Gaucher disease. *Acta Paediatr Jpn* 40(4):374–377.
24. Murphy KE, Cottle L, Gysbers AM, Cooper AA, Halliday GM (2013) ATP13A2 (PARK9) protein levels are reduced in brain tissue of cases with Lewy bodies. *Acta Neuropathol Commun* 1(1):11.
25. Dehay B, et al. (2012) Loss of P-type ATPase ATP13A2/PARK9 function induces general lysosomal deficiency and leads to Parkinson disease neurodegeneration. *Proc Natl Acad Sci USA* 109(24):9611–9616.
26. Ramonet D, et al. (2012) PARK9-associated ATP13A2 localizes to intracellular acidic vesicles and regulates cation homeostasis and neuronal integrity. *Hum Mol Genet* 21(8):1725–1743.
27. Fearnley JM, Lees AJ (1991) Ageing and Parkinson's disease: Substantia nigra regional selectivity. *Brain* 114(Pt 5):2283–2301.
28. Rieker C, et al. (2011) Neuropathology in mice expressing mouse alpha-synuclein. *PLoS ONE* 6(9):e24834.
29. Shimshek DR, Schweizer T, Schmid P, van der Putten PH (2012) Excess α-synuclein worsens disease in mice lacking ubiquitin carboxy-terminal hydrolase L1. *Sci Rep* 2:262.
30. Devine MJ, Gwinn K, Singleton A, Hardy J (2011) Parkinson's disease and alpha-synuclein expression. *Movement Dis* 26(12):2160–2168.
31. Drolet RE, Behrouz B, Lookingland KJ, Goudreau JL (2004) Mice lacking alpha-synuclein have an attenuated loss of striatal dopamine following prolonged chronic MPTP administration. *Neurotoxicology* 25(5):761–769.
32. Ubhi K, et al. (2010) Alpha-synuclein deficient mice are resistant to toxin-induced multiple system atrophy. *Neuroreport* 21(6):457–462.
33. Giasson BI, et al. (2002) Neuronal alpha-synucleinopathy with severe movement disorder in mice expressing A53T human alpha-synuclein. *Neuron* 34(4):521–533.
34. Lee MK, et al. (2002) Human alpha-synuclein-harboring familial Parkinson's disease-linked Ala-53 → Thr mutation causes neurodegenerative disease with alpha-synuclein aggregation in transgenic mice. *Proc Natl Acad Sci USA* 99(13):8968–8973.
35. Gegg ME, et al. (2012) Glucocerebrosidase deficiency in substantia nigra of parkinson disease brains. *Ann Neurol* 72(3):455–463.
36. Murphy KE, et al. (2014) Reduced glucocerebrosidase is associated with increased α-synuclein in sporadic Parkinson's disease. *Brain* 137(Pt 3):834–848.
37. Osellame LD, et al. (2013) Mitochondria and quality control defects in a mouse model of Gaucher disease—Links to Parkinson's disease. *Cell Metab* 17(6):941–953.
38. Ginns EI, et al. (2014) Neuroinflammation and α-synuclein accumulation in response to glucocerebrosidase deficiency are accompanied by synaptic dysfunction. *Mol Genet Metab* 111(2):152–162.
39. Goker-Alpan O, Stubblefield BK, Giasson BI, Sidransky E (2010) Glucocerebrosidase is present in α-synuclein inclusions in Lewy body disorders. *Acta Neuropathol* 120(5): 641–649.
40. Yap TL, et al. (2011) Alpha-synuclein interacts with Glucocerebrosidase providing a molecular link between Parkinson and Gaucher diseases. *J Biol Chem* 286(32):28080–28088.
41. Ron I, Rapaport D, Horowitz M (2010) Interaction between parkin and mutant glucocerebrosidase variants: A possible link between Parkinson disease and Gaucher disease. *Hum Mol Genet* 19(19):3771–3781.
42. Lesage S, et al.; French Parkinson's Disease Genetics Study Group (2011) Large-scale screening of the Gaucher's disease-related glucocerebrosidase gene in Europeans with Parkinson's disease. *Hum Mol Genet* 20(1):202–210.
43. Sun Y, et al. (2010) Specific saposin C deficiency: CNS impairment and acid beta-glucosidase effects in the mouse. *Hum Mol Genet* 19(4):634–647.
44. Nixon RA (2013) The role of autophagy in neurodegenerative disease. *Nat Med* 19(8): 983–997.
45. Najim al-Din AS, Wriekat A, Mubaidin A, Dasouki M, Hiari M (1994) Pallido-pyramidal degeneration, supranuclear upgaze paresis and dementia: Kufor-Rakeb syndrome. *Acta Neurol Scand* 89(5):347–352.
46. Ramirez A, et al. (2006) Hereditary parkinsonism with dementia is caused by mutations in ATP13A2, encoding a lysosomal type 5 P-type ATPase. *Nat Genet* 38(10): 1184–1191.
47. Usenovic M, Tresse E, Mazzulli JR, Taylor JP, Krainc D (2012) Deficiency of ATP13A2 leads to lysosomal dysfunction, α-synuclein accumulation, and neurotoxicity. *J Neurosci* 32(12):4240–4246.
48. Sevlever D, Jiang P, Yen SH (2008) Cathepsin D is the main lysosomal enzyme involved in the degradation of alpha-synuclein and generation of its carboxy-terminally truncated species. *Biochemistry* 47(36):9678–9687.
49. Sun Y, et al. (2010) Neuronopathic Gaucher disease in the mouse: Viable combined selective saposin C deficiency and mutant glucocerebrosidase (V394L) mice with glucosylsphingosine and glucosylceramide accumulation and progressive neurological deficits. *Hum Mol Genet* 19(6):1088–1097.
50. Maniwang E, Tayebi N, Sidransky E (2013) Is Parkinson disease associated with lysosomal integral membrane protein type-2?: Challenges in interpreting association data. *Mol Genet Metab* 108(4):269–271.
51. Blanz J, et al. (2008) Reversal of peripheral and central neural storage and ataxia after recombinant enzyme replacement therapy in alpha-mannosidosis mice. *Hum Mol Genet* 17(22):3437–3445.